

Synthesis and Characterization of Fluorene-Based Polybenzimidazole Copolymer for Gas Separation

Jun Young Han,¹ Ju Yeon Lee,¹ Hyoung-Juhn Kim,¹ Man-Ho Kim,² Su Gyeong Han,²
Jong Hyun Jang,¹ Eun Ae Cho,¹ Sung Jong Yoo,¹ Dirk Henkensmeier¹

¹Fuel Cell Research Center, Korea Institute of Science and Technology, 39-1 Hawolgok-dong, Seongbuk-gu Seoul 136-791, Republic of Korea

²Advanced Analysis Center, Korea Institute of Science and Technology, 39-1 Hawolgok-dong, Seongbuk-gu Seoul 136-791, Republic of Korea

Correspondence to: H.-J. Kim (E-mail: hjkim25@kist.re.kr) and M.-H. Kim (E-mail: man-hokim@kist.re.kr)

ABSTRACT: The purpose of this study is to develop new cardo-polybenzimidazole (CPBI) copolymers containing cardo fluorene, with improved gas permeability, specifically oxygen permeability. The characteristics of these copolymers are investigated by Fourier transform infrared spectroscopy, nuclear magnetic resonance, ¹H and ¹³C, thermo-gravimetric analysis, and wide-angle X-ray diffraction. These membranes fabricated from copolymers have relatively high oxygen diffusion coefficients, determined using gas permeation. In particular, the CPBI-co91 (synthesized by using the monomers ratio containing dibenzoic acid = 9 : 1) membrane have oxygen permeability coefficient (P_{O_2}) of 10.69 Barrer, theoretical selectivity of 5.4 for oxygen to nitrogen, and O_2 diffusion coefficient of $9.64 \times 10^{-8} \text{ cm}^2/\text{s}$. © 2014 Wiley Periodicals, Inc. *J. Appl. Polym. Sci.* **2014**, *131*, 40521.

KEYWORDS: copolymers; membranes; separation techniques

Received 28 November 2013; accepted 28 January 2014

DOI: 10.1002/app.40521

INTRODUCTION

Polymeric membranes offer several advantages for gas separation, and as a result, their use in these applications is growing rapidly. These advantages include smaller equipment than with conventional methods, high energy efficiency, easy collection of byproducts, and low production cost resulting from innovative designs and process development.¹ Polymers that are chemically and mechanically stable at high temperatures and pressures have been studied for gas separation applications such as carbon dioxide capture and hydrogen separation from mixed gases.^{1–5} Examples of such polymers are polybenzothiazoles (PBTs), polybenzoxazoles (PBOs), and polybenzimidazoles (PBIs).^{2–4}

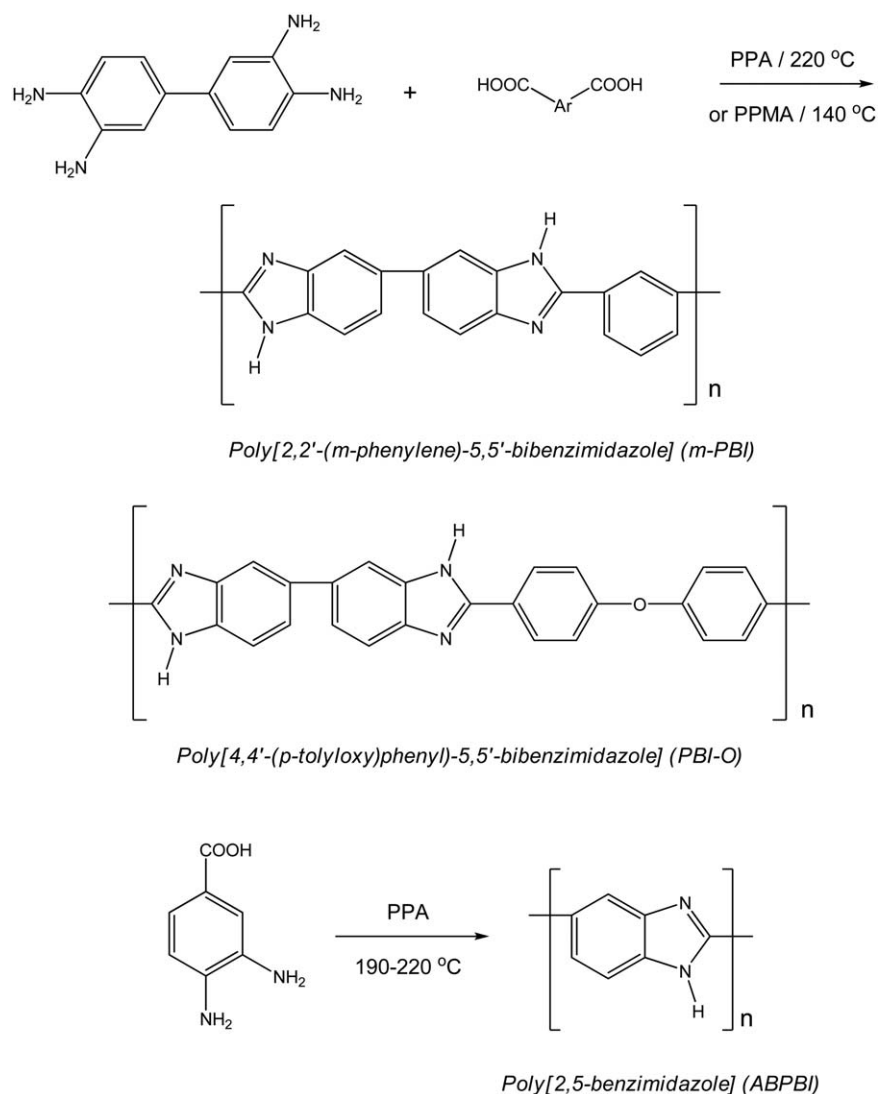
OBIGGS (On Board Inert Gas Generation System) is a system that generates nitrogen from the atmosphere to provide an inert gas blanket for safe filling of aircraft fuel tanks. To prevent the ignition of the fuel, the oxygen level must be below 12%. This is easily achievable with the OBIGGS, which is equipped with a membrane capable of delivering an exit stream containing 95/5 (v/v%) nitrogen/oxygen, as well as a second exit stream enriched in oxygen.⁵ Such a membrane system offers the following advantages over alternative devices: unlimited nitrogen supply, no chemicals, low weight system, low life

cycle cost, and negligible impact on logistics.^{5,6} Membranes used in the OBIGGS must have high permeability, along with high selectivity for efficient separation of O_2 and N_2 . In addition, the membrane must be able to operate at a minimum temperature of 90°C, to withstand the heat generated by aircraft engines.⁶

PBIs are a group of membrane polymers that can be manufactured by condensation polymerization between a monomer with four amine groups, such as 3,3'-diaminobenzidine (DAB), and one of several other suitable monomers, e.g., isophthalic acid, terephthalic acid, 4,4'-oxybis(benzoic acid), or diphenyl isophthalate (Scheme 1).^{7–9} Alternatively, poly(2,5-benzimidazole) (ABPBI, Scheme 1) offers excellent mechanical strength, and it can be made from a single monomer using a simple synthetic method.¹⁰ However, the extremely high crystallinity of this polymer renders it insoluble in most organic solvents. Despite their excellent thermal resistance and mechanical properties, PBIs have seen only limited use as gas separation membranes. This is because of their dense chain packing, a consequence of hydrogen bonding between the hydrogen and nitrogen atoms of the imidazole rings of adjacent polymer chains.^{11,12} Although the dense packing strengthens the polymer structure, it leads to low gas permeability, a disadvantage in gas separation

Additional Supporting Information may be found in the online version of this article.

© 2014 Wiley Periodicals, Inc.



Scheme 1. Synthesis of PBI derivatives; polyphosphoric acid (PPA), phosphorus pentoxide, and methanesulfonic acid mixture (PPMA).

applications.^{11,13–15} To improve permeability, many researchers have studied modification of the functional groups on the polymer backbone, branch to increase the free volume between polymer chains, surface modification, and polymer blends.^{11,14–19}

The purpose of this study was to develop a new PBI separation membrane with improved gas permeability, specifically oxygen permeability, for application in OBIGGS. This was achieved using a monomer that could form a structure similar to that of polymers with intrinsic microporosity (PIMs), leading to large free volume. Specifically, copolymers of monomer containing fluorene (having the cardo structure) and one of several other monomers were synthesized, and the effect of the ratio of the two monomers on gas permeability was determined using a time-lag method.

EXPERIMENTAL

Materials

DAB, isophthalic acid (IPA), 4,4'-oxybis(benzoic acid) (OBBA), 115% polyphosphoric acid (PPA), anhydrous *N*-methyl-2-pyrrolid-

one (NMP), methanesulfonic acid, phosphorous pentoxide (P_2O_5), fluorene, 4-fluorobenzonitrile, 18-crown-6-ether, K_2CO_3 , KOH, tetrahydrofuran (THF), DMF, toluene, HCl, acetic acid, hexane, 12% ammonia water, and ethanol were purchased from Sigma-Aldrich and Baker and used without further purification.

Synthesis of 9,9'-bis(4-cyanophenyl)fluorene

Fluorene (20.0 g, 120.3 mmol), 4-fluorobenzonitrile (32.5 g, 268.3 mmol), potassium carbonate (39.6 g, 286.0 mmol), 18-crown-6-ether (16.4 g, 62 mmol), 30 mL of toluene, and 100 mL of DMF were mixed in a 500 mL 3-neck round bottom flask for 20 h at 140°C under an argon gas atmosphere. Afterward, the mixture was cooled to room temperature, and then it was poured into 1,400 mL of ice water to obtain a fine powder. The powder was purified by recrystallization with tetrahydrofuran (THF) and then the recrystallized material was washed with a small amount of hexane,²⁰ and 20.7 g (46.7% yield) of 9,9'-bis(4-cyanophenyl)fluorene were obtained. Its properties were: melting point (mp) of 284–286°C²⁰; IR (ATR) 2229 cm^{-1}

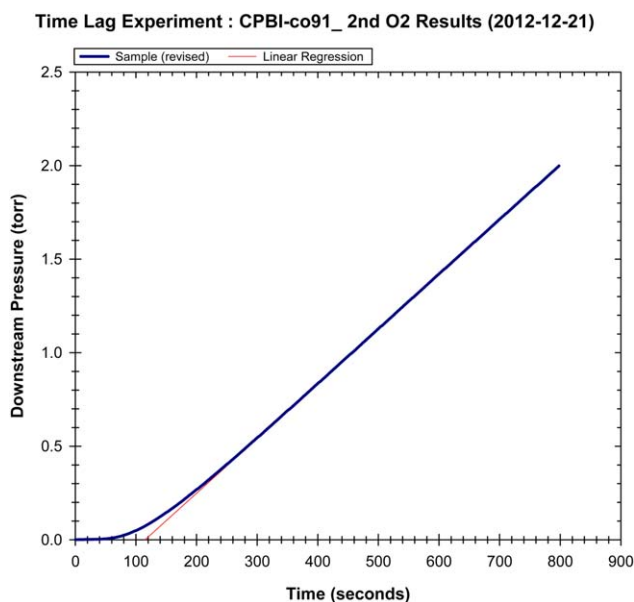


Figure 1. Gas permeation time-lag graph. [Color figure can be viewed in the online issue, which is available at wileyonlinelibrary.com.]

(C≡N stretch); ^1H NMR (300 MHz, DMSO- d_6 , δ): 7.28–7.31 (d, 4H), 7.33–7.39 (t, 2H), 7.44–7.50 (m, 4H), 7.74–7.78 (d, 4H), 7.98–8.01 (d, 2H).

Synthesis of 9,9'-bis(4-carboxyphenyl)fluorene (9BCPF)

9,9'-bis(4-cyanophenyl)fluorene (17.5 g, 47.5 mmol), potassium hydroxide (37.3 g, 664.6 mmol), 120 mL of ethanol, and 120 mL of deionized water were mixed for four days at reflux temperature. After cooling to room temperature, the reaction mixture was acidified with hydrochloric acid to obtain a precipitate. The precipitate was collected, washed with water, and then recrystallized using acetic acid to obtain 13.6 g (70.4% yield) of 9BCPF as white crystals.²⁰ Its properties were: mp 359–360°C²⁰; IR (ATR): 1690 cm^{-1} (C=O stretch), 2700–3200 cm^{-1} (O—H stretch); ^1H NMR (300 MHz, DMSO- d_6 , δ): 7.22–7.25 (d, 4H), 7.32–7.37 (t, 2H), 7.42–7.49 (m, 4H), 7.84–7.87 (d, 4H), 7.96–7.98 (d, 2H), 12.90 (s, 2H, OH); ^{13}C NMR (300 MHz, DMSO- d_6 , δ): 65.5, 121.28, 126.53, 128.28, 128.63, 129.93, 130.05, 140.13, 149.83, 150.54, 167.43 (C=O).

Synthesis of Cardo-PBI Homopolymer (CPBI-homo)

DAB (3.0 g, 14.0 mmol) and 9BCPF (5.7 g, 14.0 mmol) were placed in round bottom flask with Eaton's reagent, and then stirred for 1 h at 80°C under an argon atmosphere. Afterward, the reaction temperature was slowly increased to 140°C then the reactor contents were stirred for 2 h. The polymer was precipitated in deionized water, and then washed for three days with 12% ammonia water at 60°C to remove residual phosphoric acid. The polymer was washed with water to neutral pH followed by drying in a 60°C vacuum oven to obtain the CPBI-homo.

Synthesis of Cardo-PBI Copolymer (CPBI-coXY)

The synthetic method for 9 : 1 copolymer is given as representative, DAB (3.0 g, 14.0 mmol), 9BCPF (5.1 g, 12.6 mmol), and 4,4'-oxybis(benzoic acid) (OBBA) (362 mg, 1.4 mmol) were added to a mixture of Phosphorus pentoxide and Methanesul-

fonic acid in round bottom flask, then stirred for 1 h at 80°C under an argon gas atmosphere. Afterward, the reaction temperature was slowly increased to 140°C, then the reactor contents were stirred for 2 h. Subsequently, the method of obtaining polymer was identical to that used in the preparation of CPBI-homo. The copolymer was named as CPBI-coXY (X : Y = 9BCPF : OBBA molar ratio, X + Y = 10), according to molar ratio of 9BCPF to OBBA.

Fabrication of PBI Membrane for Gas Separation

Polymer membranes for measurement of gas permeation were fabricated via a solution casting method. Using *N*-methyl-2-pyrrolidone (NMP) as the solvent, the CPBI polymer was dissolved to 3 wt % at room temperature. After filtering through a 0.45 μm syringe filter, the solution was applied to a glass plate, and then dried in an 80°C vacuum oven for over a day and at 100°C for two days in a vacuum, to obtain a brown transparent membrane of 40–50 μm thickness. Thereafter, the membranes were soaked in methanol to remove any residual solvent in the membrane for one day. Finally, the membranes to measure were obtained by drying in 80°C vacuum oven for a day.

Characteristics of Monomers and Polymers

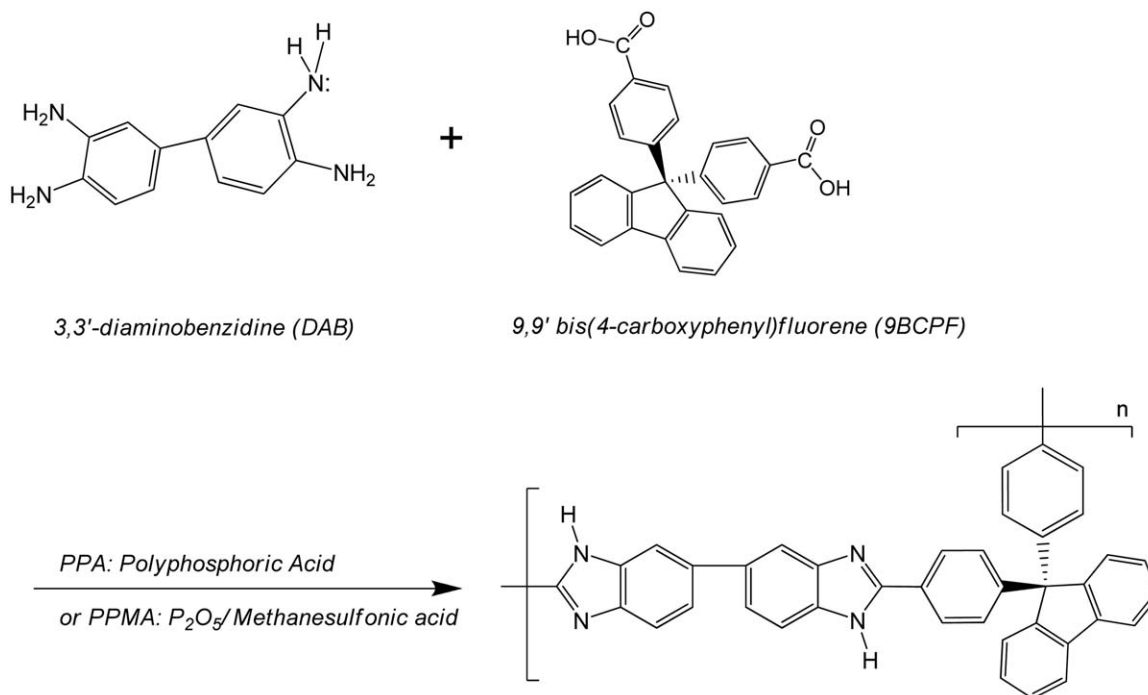
Functional groups of each monomer and polymer were verified using FTIR (Spectrum 100 Series, PerkinElmer, UK). Structures of the monomers and polymers were examined using NMR (Bruker, 300 MHz). Thermal characteristics of the membranes were evaluated using thermo-gravimetric analysis (TGA) (Universal V4.2E TA Instruments, 2050 TGA). The analysis was performed under a nitrogen atmosphere, and the temperature was increased at rate of 10°C/min up to 1000°C. The CPBI molecular weight was determined by gel permeation chromatograph (GPC) using a Waters GPC system. The column was filled with 2 \times TSKgel α -M (7.8 \times 300 mm) using NMP as an eluent with addition of 0.05M LiBr. The eluent pumping rate (Waters 515) was 1.0 mL/min and the temperature was 45°C. PPMA was used as a standard. Detection was accomplished using a Waters 410 differential refractometer.

X-ray Measurement

The intermolecular distances in membranes (CPBI, m-PBI, and PBI-O) were measured with a wide angle X-ray diffractometer (WAXD, model: EMPYREAN diffractometer, PANalytical) in a continuous scan mode using CuK α 1 radiation at 45 kV and 40 mA. The angular range was $2\theta = 10^\circ$ – 90° with a step size of 0.01°. The intermolecular distances were obtained from Bragg's law.

Measurement of Gas Permeability

The gas permeability of the CPBI membranes was measured at 30°C and feed pressure 1005 Torr. The downstream pressure for the time-lag was measured at intervals of every 2 s from vacuum state to 2 Torr, using an automated gas permeation system (GPTS-AIRRANE, Korea). The system included a thermostatically controlled chamber for maintaining isothermal conditions. The effective membrane area (A) was 14.50 cm^2 , and on the downstream side, the buffer volume was 70 cm^3 . The unit was equipped with a capacitance manometer for pressure measurement (Type 626, Baratron®, MKS Instruments, USA). Prior to the measurement, both the upstream and downstream sides of the membrane were degassed for at least 8 h at the operating



Scheme 2. Synthesis of cardo-PBI homopolymer (CPBI-homo).

temperature. The polymer membrane was attached to the permeation cell, and then both sides of the membrane were degassed using a vacuum pump (GLD-136C, ULVAC KIKO, Japan). At the initial time ($t = 0$), the gas of interest (O_2 , N_2 , or CO_2) was injected at the top of the membrane at constant pressure (P_{feed}). The time-lag graph (Figure 1) was obtained by measuring the pressure at bottom of the membrane as a function of time.

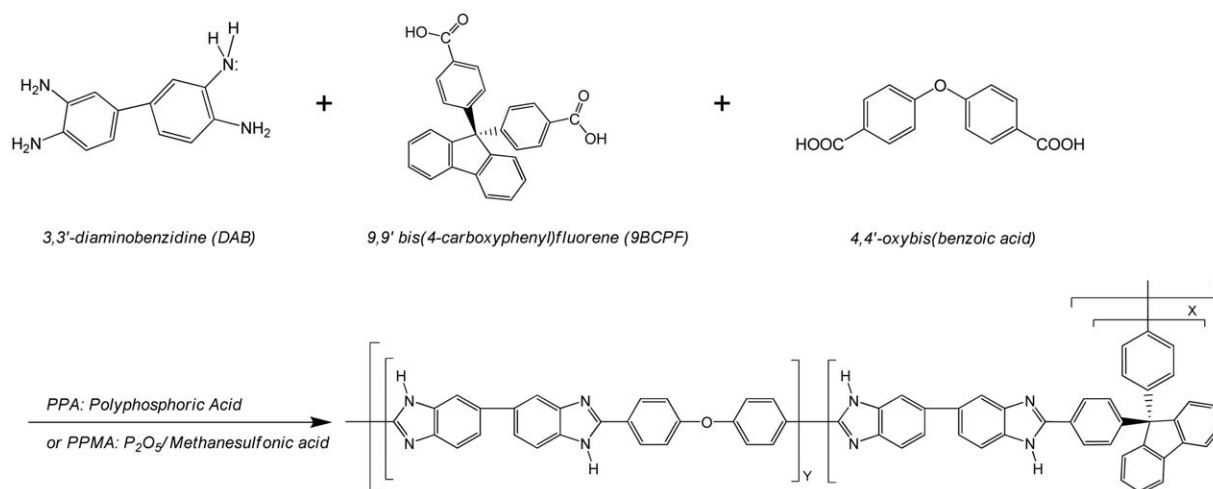
RESULTS AND DISCUSSION

Synthesis of 9,9'-bis(4-carboxyphenyl)fluorene

9,9'-Bis(4-cyanophenyl)fluorene was synthesized by nucleophilic substitution reaction.²⁰ The two hydrogen atoms at the carbon

9 in fluorene were replaced by 4-cyanophenyl groups through *N*-substitution. The substitution was confirmed by $^1\text{H-NMR}$ (300 MHz, $\text{DMSO-}d_6$), which shows no hydrogen atoms (chemical shift 3.92 ppm, 2H) at carbon 9 of the substituted fluorene.

9,9'-Bis(4-carboxyphenyl)fluorene (9BCPF) was synthesized from 9,9'-bis(4-cyanophenyl)fluorene by the hydrolysis reaction.²⁰ The hydrolysis was confirmed by $^1\text{H-NMR}$, $^{13}\text{C-NMR}$, and FTIR (Noted in the Supporting Information). That is, the hydrogen atoms of the carboxylic acid groups of 9BCPF can be found at 12.87 ppm in $^1\text{H-NMR}$ result, and the aromatic protons of 9BCPF were detected in the region between 7.2 and 8.0 ppm. Also the chiral carbon and $\text{C}=\text{O}$ carbon peak in the ^{13}C NMR spectra were appeared at 65.5 and 167.4 ppm,



Scheme 3. Synthesis of CPBI-coXY copolymer with oxygen in backbone structure ($X + Y = 10$, $X = 5-9$).

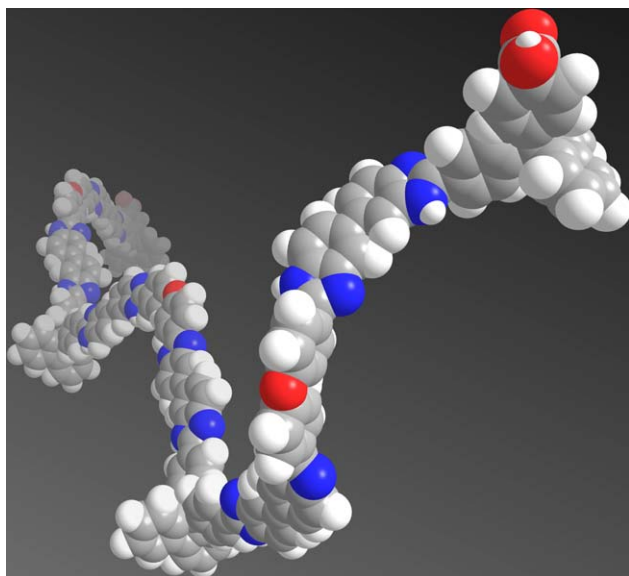


Figure 2. Structure of CPBI-coXY polymer. [Color figure can be viewed in the online issue, which is available at wileyonlinelibrary.com.]

respectively. Moreover, in FTIR results, the band at 2229 cm^{-1} for $\text{—C}\equiv\text{N}$ in 9,9'-bis(4-cyanophenyl)fluorene disappeared, and strong CO stretching bands appeared at 1683 and 1273 cm^{-1} .

Synthesis of CPBI Homopolymer and CPBI Copolymer

As shown in Scheme 2, cardo-polybenzimidazole (CPBI) homopolymer was synthesized from DAB and 9BCPF, using Eaton's reagent as the reaction solvent. Gelling, observed during the polymerization reaction, was minimized by adjusting the ratio of phosphorus pentoxide to Methanesulfonic acid (PPMA, $\text{P}_2\text{O}_5/\text{CH}_3\text{SO}_3\text{H}$). The weight-average molecular weight (M_w) of the CPBI-homo was about 241 kDa. Unfortunately, the homopolymer was weak and fragile, so that its permeability could not be measured because it was damaged when placed in the measuring cell. To improve the strength of the membrane, 4,4'-oxybis(benzoic acid) (OBBA) was selected as a monomer (Scheme 3), and the resulting polymer showed good mechanical characteristics for gas permeation test.^{7,8} The CPBI copolymer (CPBI-coXY) structure is shown in Scheme 3 and Figure 2.

Figure 3 shows $^1\text{H-NMR}$ (300 MHz, $\text{DMSO-}d_6$) spectra of the CPBI-homo, CPBI-coXY copolymers, and PBI-O. The hydrogen atom of the OBBA unit, which is not seen in the CPBI homopolymer, appears at 7.30, 7.87, and 8.30 ppm in the copolymers, and the peak increases with the relative amount of OBBA. In the FTIR spectra shown in Figure 4, the C—O—C stretching absorption peak of CPBI-co55 at 1169 and 1235 cm^{-1} does not appear in the CPBI trace. In summary, both the $^1\text{H-NMR}$ and FTIR results are consistent with the proposed structures of CPBI and the other polymers studied.

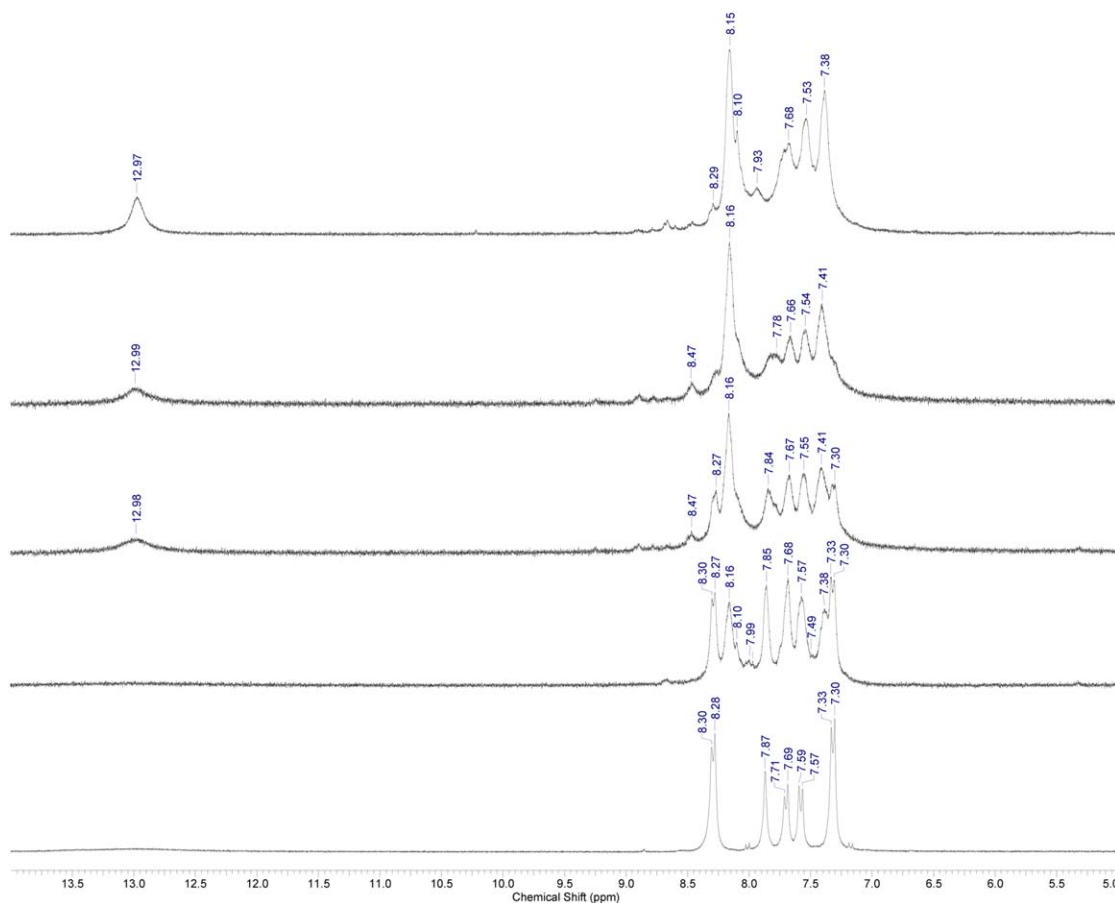


Figure 3. $^1\text{H-NMR}$ (300 MHz, $\text{DMSO-}d_6$) spectra of CPBI-homo, CPBI-coXY and PBI-O. [Color figure can be viewed in the online issue, which is available at wileyonlinelibrary.com.]

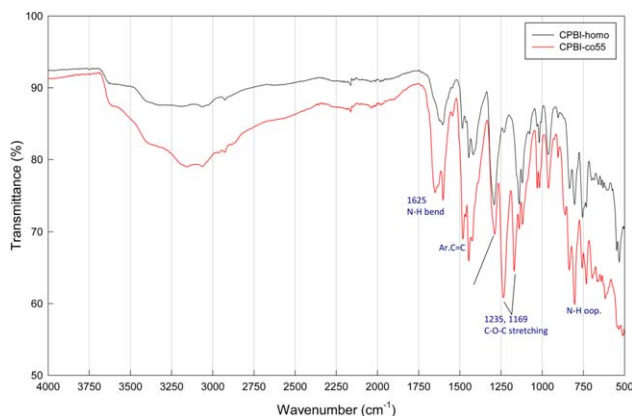


Figure 4. FTIR spectra of CPBI and CPBI-co55 membranes. [Color figure can be viewed in the online issue, which is available at wileyonlinelibrary.com.]

Physical Properties

TGA was performed to evaluate the thermal characteristics of the membranes. The results are shown in Figure 5 and Table I. Mass continuously decreased with increasing temperature up to about 150°C as moisture evaporated from the polymer. Decomposition of polymer occurred near 260°C, as indicated by T_i (Table I), the temperature at which the slope changes significantly. T_i decreased with an increased relative amount of OBBA in the polymer backbone, but the effect was not large.

As given in Table I, the onset point temperature (OPT, TA Universal Analysis Program, T_{OPT} in Figure 5) were in the range of 343–382°C, the residue (char yield) was about 74 wt % for all copolymers tested. Meanwhile, as can be seen in Figure 5, the four inflection points above 300°C can be related to the structure of the polymer chain. That is, as the relative amount of OBBA in the copolymer increased, the OPT decreased. In summary, the TGA results presented here suggest that continuous use of the CPBI polymers at up to 200°C is acceptable because T_i is near upon 260°C.

As illustrated in Figure 6, all of the PBI membranes had an amorphous polymer structure. The average intermolecular spacing distance (d -spacing) values were calculated using the Bragg equation ($d = \lambda/2\sin\theta$) and are summarized in Table I. Even

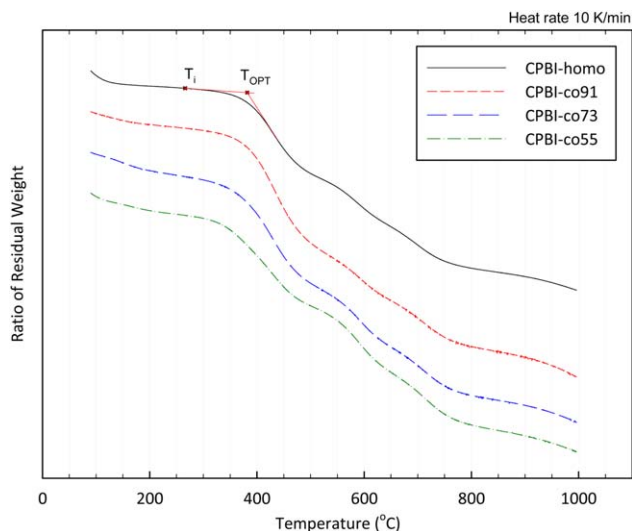


Figure 5. TGA thermograms of CPBI and CPBI-coXY membranes under nitrogen atmosphere. [Color figure can be viewed in the online issue, which is available at wileyonlinelibrary.com.]

though inclusion of the fluorene group increased the mass of the homopolymer PBI-O by more than 50%, the d -spacing (Å) did not change significantly. However, CPBI-co91 membrane had the largest average d -spacing, 5.015 Å. Generally, fractional free volume (FFV) is influenced by the chain mobility, packing density, and side groups, and it has a direct relationship with diffusivity. Permeation of gases through the polymer membrane was interpreted as a function of diffusion coefficient D and solubility coefficient S . The diffusion coefficient was determined from the FFV and chain mobility inside the polymer membrane, and solubility was determined from the interaction between the gas molecules and the polymer.²¹ The slightly increased d -spacing is expected to increase as a result of the FFV and the gas permeability as a whole.²²

Gas Permeation Properties

Table II shows the results of gas permeation experiments and ideal permselectivities (α) for the CPBI copolymer, m-PBI, and PBI-O as gas separation membranes. In addition, gas diffusion coefficients (D), solubility coefficients (S), diffusion selectivity (α_D), and solubility selectivity (α_S) values are summarized in

Table I. Physical Characteristics of the Fabricated CPBI, CPBI-coXY, and Other PBI Membrane

Item	T_i (IDT, °C) ^a	T_{OPT} (°C) ^b	T_{900} (wt %) ^c	M_n ^d	M_w ^e	d -spacing (Å)
CPBI-homo	266	382	77.6	9,445	241,338	-
CPBI-co91	260	381	73.5	10,165	164,318	5.015
CPBI-co73	260	371	73.3	6237	93,947	4.524
CPBI-co55	254	343	74.4	12,943	1,073,290	4.354
m-PBI	333	404	84.0	27,746	289,697	3.686
PBI-O	293	357	75.5	25,023	140,494	4.657

^a Initial decomposition temperature (IDT).

^b Onset point temperature.

^c Char yield at 900°C.

^d Number average molecular weight.

^e Weight average molecular weight.

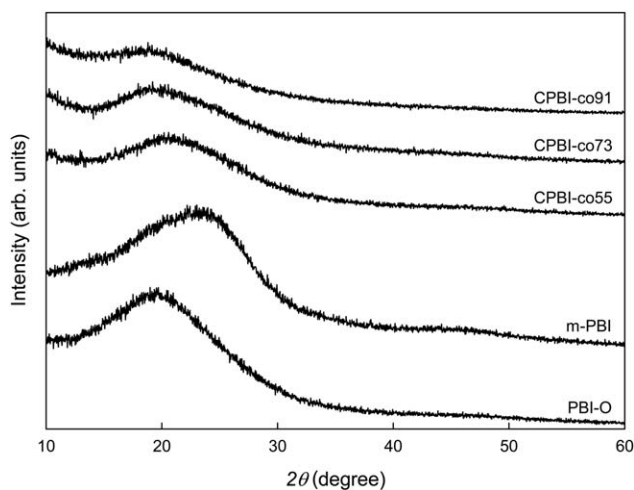


Figure 6. Wide-angle X-ray diffraction (WAXD) results on prepared CPBI-coXY, m-PBI, and PBI-O membranes.

Table III. The gas permeability coefficients (also shown in Figure 7) were obtained at 30°C and 1005 Torr for all membranes except m-PBI, which was tested at 4000 Torr because of very low permeability. The selectivity coefficients for O₂/N₂, CO₂/N₂, and CO₂/O₂ were calculated from the permeability test results. The diffusion coefficients were calculated from the time-lag (gas flow vs. time plot) in the program ($D = d^2/\theta$, noted in the Supporting Information). In summary, the gas permeability coefficient was increased with increase in the ratio of 9BCPF including fluorene unit. Especially, CPBI-co91 copolymer

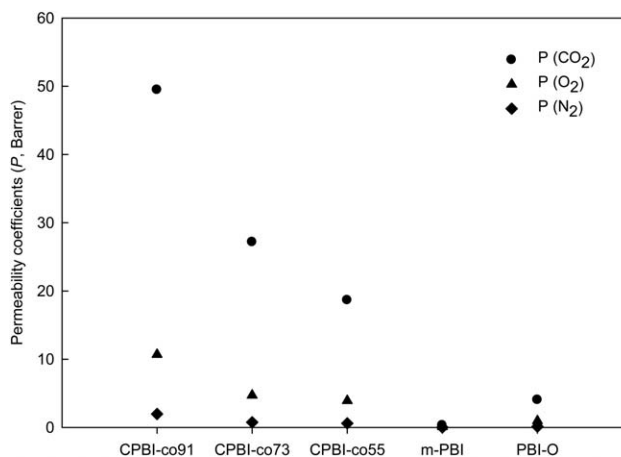


Figure 7. Pure gas permeability coefficients (P) for the each PBI membrane (CPBI-coXY, m-PBI, and PBI-O).

membrane had oxygen permeability coefficient (P_{O_2}) of 10.69 Barrer, theoretical selectivity of 5.40 for oxygen to nitrogen, and also O₂ diffusion coefficient of $9.64 \times 10^{-8} \text{ cm}^2/\text{s}$.

Gas permeability coefficients (P) were dependent on the molar ratio of 9BCPF to OBBA in the copolymer chain. That is, for CPBI-coXY gas permeability followed the order with the increase of the 9BCPF, CPBI-co55 < CPBI-co73 < CPBI-co91. Also, for all PBIs the P increased with decreasing kinetic diameter of the gas molecule, following the order CO₂ (kinetic diameter: 3.3 Å) > O₂ (3.46 Å) > N₂ (3.64 Å).²³ However, the diffusion

Table II. Gas Permeability Coefficients (P)^a and Ideal Permselectivities (α)^b of CPBI-coXY, m-PBI, and PBI-O membranes

Membrane	$P(\text{CO}_2)$	$P(\text{O}_2)$	$P(\text{N}_2)$	$\alpha(\text{O}_2/\text{N}_2)$	$\alpha(\text{CO}_2/\text{N}_2)$	$\alpha(\text{CO}_2/\text{O}_2)$
CPBI-co91	49.47	10.69	1.97	5.40	24.00	4.62
CPBI-co73	27.16	4.71	0.76	6.14	35.48	5.77
CPBI-co55	18.64	3.92	0.61	6.40	30.45	4.75
m-PBI	0.304	0.099	0.011	8.86	27.25	3.07
PBI-O	4.03	0.96	0.11	8.72	36.63	4.19

^aPure gas permeability in Barrer ($1 \text{ Barrer} = 10^{-10} \text{ cm}^3(\text{STP}) \text{ cm Hg}^{-1} \text{ cm}^{-2} \text{ s}^{-1}$), measured at 30°C and 1005 Torr, except m-PBI, which was measured at 4000 Torr.

^bRatio of the individual gas permeabilities, $\alpha(A/B) = P(A)/P(B)$.

Table III. Gas Diffusion Coefficients (D), Solubility Coefficients (S), Diffusion Selectivities (α_D), and Solubility Selectivities (α_S) of CPBI-coXY, m-PBI, and PBI-O at 30°C

Membrane	$D (10^{-8} \text{ cm}^2/\text{s})$			$S (10^{-2} \text{ cm}^3 (\text{STP})/\text{cm}^3 \text{ cm Hg})^a$			α_D			α_S		
	CO ₂	O ₂	N ₂	CO ₂	O ₂	N ₂	O ₂ /N ₂	CO ₂ /N ₂	CO ₂ /O ₂	O ₂ /N ₂	CO ₂ /N ₂	CO ₂ /O ₂
CPBI-co91	5.29	9.64	2.22	9.352	1.109	0.887	4.342	2.383	0.549	1.250	10.538	8.433
CPBI-co73	1.79	7.91	0.913	15.173	0.595	0.832	8.664	1.961	0.226	0.715	18.228	25.482
CPBI-co55	1.83	3.76	0.728	10.186	1.043	0.838	5.165	2.514	0.487	1.244	12.156	9.770
m-PBI	0.093	0.244	0.035	3.269	0.406	0.314	6.971	2.657	0.381	1.291	10.401	8.056
PBI-O	0.404	1.43	0.231	9.975	0.671	0.476	6.190	1.749	0.283	1.410	20.948	14.859

^aThe solubility coefficient is calculated from $P = D \times S$.

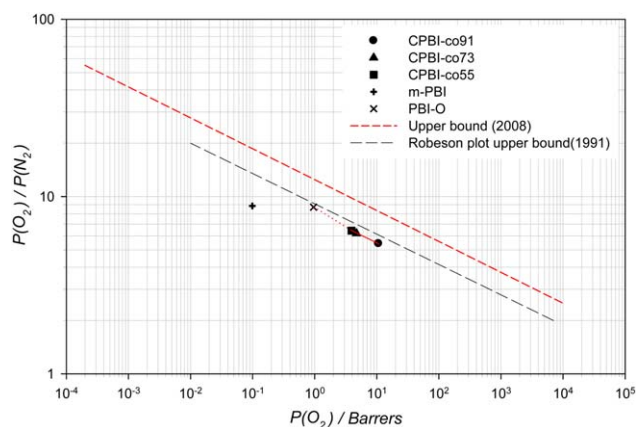


Figure 8. Robeson plot of O_2/N_2 selectivity as a function of O_2 permeability coefficient. [Color figure can be viewed in the online issue, which is available at wileyonlinelibrary.com.]

coefficients followed the order $D(O_2) > D(CO_2) > D(N_2)$, as shown in Table III. Even though the kinetic diameter of the O_2 molecule is larger than that of CO_2 , the latter has a lower diffusivity because of interaction between CO_2 and the polar groups in the polymer chain, which means that CO_2 in the membrane has a larger solubility at the same operating conditions.^{24–26} CPBI-co91 had the highest diffusion coefficient, as well as the highest permeability for all gases. Interestingly, this copolymer had relatively a higher diffusivity and a lower O_2 solubility coefficient than fluorinated polyimides and poly(ether imide)s prepared by other laboratories.^{24,25} The gas permeability coefficient increased by more than a factor of two with an increase in the proportion of the 9BCPF monomer, which shows the effect of increased gas diffusion in the polymer structure attributable to the fluorene unit. The increase in FFV afforded by the fluorene moiety in the polymer chain also contributed to the increase in gas permeability, but the effect of diffusivity was probably more important because the effect of diffusion on overall permeability is known to be dominant.²¹ While the permeability of CPBI-co73 was lower than that of CPBI-co91, the former had higher values of ideal permselectivity and solubility selectivity of CO_2 .

The results of $P(O_2)/P(N_2)$ versus $P(O_2)$ are shown in Figure 8 using Robeson plot.^{27,28} The data nearly approach the line suggested by Robeson.²⁷ The O_2 permeability and selectivity is expected to follow the solid line corresponding to the change in the ratio of 9BCPF to OBBA.

CONCLUSIONS

Polybenzimidazole derivatives with new structures were synthesized using 9BCPF including fluorene as a monomer. In particular, CPBI-co91 copolymer membrane has a higher d-spacing, oxygen permeability, and diffusion coefficient, a lower solubility coefficient for O_2 , and a high selectivity (considering permeability) for O_2 over N_2 when compared to PBI polymers in general. These copolymers backbone that can form three-dimensional structure in polymer is created by fluorene unit, which causes increase in openness between polymer chains. The gas perme-

ability coefficient was increased with increase in the ratio of monomers including fluorene unit. As a result of these improved properties, these polymer derivatives are expected to have extremely high usability for separation of O_2 and N_2 for OBIGGS.

ACKNOWLEDGMENTS

The authors would like to thank the COE (Center of Excellence) program of the Korea Institute of Science and Technology and the WPM (World Premier Materials) program of the Ministry of Trade, Industry and Energy. They also would like to thank Dr. Su Jae Kim and Mr. Chang Yeol Park of the Neutron Science Division of HANARO for generously providing X-beam time.

REFERENCES

- Bernardo, P.; Drioli, E.; Golemme, G. *Ind. Eng. Chem. Res.* **2009**, *48*, 4638.
- Park, H. B.; Jung, C. H.; Lee, Y. M.; Hill, A. J.; Pas, S. J.; Mudie, S. T.; Van Wagner, E.; Freeman, B. D.; Cookson, D. *J. Science* **2007**, *318*, 254.
- Smith, Z. P.; Tiwari, R. R.; Murphy, T. M.; Sanders, D. F.; Gleason, K. L.; Paul, D. R.; Freeman, B. D. *Polymer* **2013**, *54*, 3026.
- Kim, S.; Lee, Y. M. *Curr. Opin. Chem. Eng.* **2013**, *2*, 238.
- Reynolds, T. L. Boeing–Seattle Phantom Works, Halon Options Technical Working Conference **2001**, 51.
- Oh, D.; Ha, S.; Lee, J.; Kim, H.; Nam, S. *KIC News* **2011**, *14*, 37.
- Leykin, A. Y.; Fomenkov, A. I.; Galpern, E. G.; Stankevich, I. V.; Rusanov, A. L. *Polymer* **2010**, *51*, 4053.
- Ueda, M.; Masaki, S.; Mochizuki, A. *Macromolecules* **1985**, *18*, 2723.
- Kumbharkar, S. C.; Nazrul Islam, M. D.; Potrekar, R. A.; Kharul, U. K. *Polymer* **2009**, *50*, 1403.
- Kim, H.-J.; Cho, S. Y.; An, S. J.; Eun, Y. C.; Kim, J.-Y.; Yoon, H.-K.; Kweon, H.-J.; Yew, K.-H. *Macromol. Rapid Commun.* **2004**, *25*, 894.
- Kumbharkar, S. C.; Kharul, U. K. *J. Membr. Sci.* **2010**, *357*, 134.
- Kumbharkar, S. C.; Kharul, U. K. *Euro. Polym. J.* **2009**, *45*, 3363.
- Pesiri, D. R.; Jorgensen, B.; Dye, R. C. *J. Membr. Sci.* **2003**, *218*, 11.
- Kumbharkar, S. C.; Karadkar, P. B.; Kharul, U. K. *J. Membr. Sci.* **2006**, *286*, 161.
- Hosseini, S. S.; Teoh, M. M.; Chung, T. S. *Polymer* **2008**, *49*, 1594.
- Kumbharkar, S. C.; Li, K. *J. Membr. Sci.* **2012**, *416*, 793.
- Rana, D.; Matsuura, T. In *Encyclopedia of Membrane Science and Technology*; Hoek, E. M. V.; Tarabara, V. V., Eds.; Wiley: New Jersey, **2013**; Vol. 3, pp 1668–1693.

18. Savoji, H.; Rana, D.; Matsuura, T.; Soltanieh, M.; Tabe, S. *J. Appl. Polym. Sci.* **2012**, *124*, 2287.
19. Han, J. Y.; Lee, W.; Choi, J. M.; Rajkumar, P.; Min, B.-R. *J. Membr. Sci.* **2010**, *351*, 141.
20. Liou, G.-S.; Yen, H.-J.; Su, Y.-T.; Lin, H.-Y. *J. Polym. Sci.: Part A* **2007**, *45*, 4352.
21. Koros, W. J.; Coleman, M. R.; Walker, D. R. B. *Annu. Rev. Mater. Sci.* **1992**, *22*, 47.
22. Pixton, M. R.; Paul, D. R. *J. Polym. Sci. Part B: Polym. Phys.* **1995**, *33*, 1135.
23. Matteucci, S.; Yampolskii, Y.; Freeman, B. D.; Pinnau, I. *Materials Science of Membranes for Gas and Vapor Separation*, Chichester: Wiley; **2006**.
24. Sen, S. K.; Dasgupta, B.; Banerjee, S. *J. Membr. Sci.* **2009**, *343*, 97.
25. Tanaka, K.; Kita, H.; Okano, M.; Okamoto, K.-I. *Polymer* **1992**, *33*, 585.
26. Tanaka, K.; Kita, H.; Okano, M.; Okamoto, K.-I. *J. Polym. Sci. Part B: Polym. Phys.* **1993**, *31*, 1127.
27. Robeson, L. M. *J. Membr. Sci.* **1991**, *62*, 165.
28. Robeson, L. M. *J. Membr. Sci.* **2008**, *320*, 390.